



FKBP5 promotes osteogenic differentiation of mesenchymal stem cells through type-I interferon pathway Inhibition

Jun Tang¹ · Ming Li¹ · Yuanquan Chen¹ · Yuwei Liang¹ · Wenbin Yan¹ · Qing Ning¹ · Hao Deng¹ · Huatao Liu¹ · Yuxi Li¹ · Lin Huang¹ 

Received: 9 October 2024 / Revised: 27 April 2025 / Accepted: 13 May 2025
© The Author(s) 2025

Abstract

The decreased osteogenesis of bone marrow mesenchymal stem cells (BMSCs) is an important factor causing bone loss. Nevertheless, its deep molecular mechanism has still not been fully clarified. To elucidate the regulatory mechanisms underlying BMSC osteogenesis, we conducted a bioinformatics screen using public datasets from the Gene Expression Omnibus (GEO) database to identify genes displaying significant expression dynamics during the osteogenic differentiation of BMSCs. We observed a significant upregulation of FK506 Binding Protein 5 (FKBP5) expression during the osteogenic differentiation of BMSCs. Besides, knockdown and overexpression of FKBP5 could reduce and increase osteogenic markers and Alizarin Red S (ARS) staining, respectively. Enrichment analysis of RNA sequencing (RNA-seq) demonstrated that downregulation of FKBP5 activated IFN α / β signaling pathway. FKBP5 overexpression relieved the inhibitory effect of IFN β on osteogenesis. In addition, one of the upregulated interferon-stimulated genes (ISG), interferon-induced protein with tetratricopeptide repeats 2 (IFIT2), negatively regulated osteogenesis of BMSCs. IFIT2 knockdown rescued negative effect on osteogenesis caused by downregulation of FKBP5. Hydroxyapatite scaffold implanted in nude mice and drilled tibiae model in C57BL/6 mice confirmed positive role of FKBP5 in osteogenesis in vivo. Therefore, we determined the beneficial effect of FKBP5 on osteogenesis of BMSCs and validated the critical role of FKBP5/IFIT2 axis in this process. These findings might contribute to comprehension and treatment of bone diseases, like osteoporosis and bone fracture.

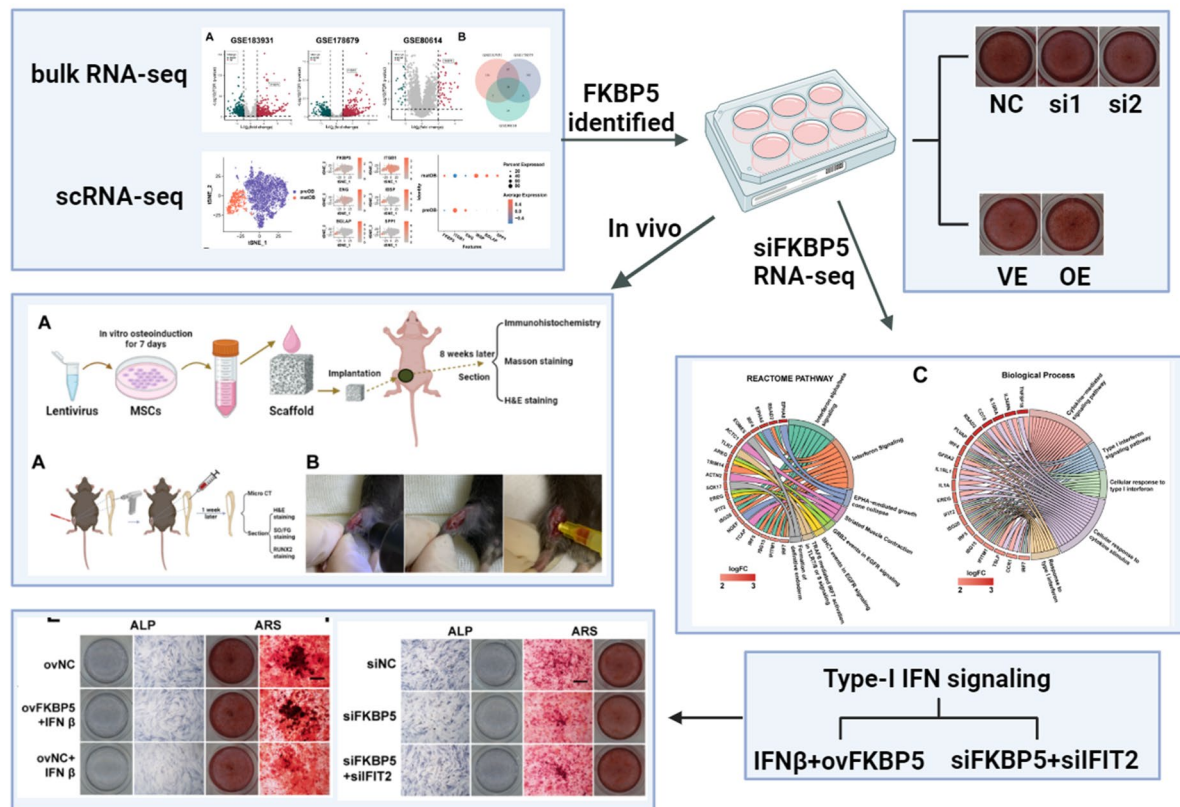
Jun Tang, Ming Li, and Yuanquan Chen are the first, second, and third co-first authors, respectively.

✉ Yuxi Li
liy73@mail.sysu.edu.cn

✉ Lin Huang
huangl5@mail.sysu.edu.cn

¹ Department of Orthopedics, Sun Yat-sen Memorial Hospital of the Sun Yat-sen University, 107 Yanjiang West Road, Yuexiu District, Guangzhou, China

Graphical abstract



Keywords Osteogenic differentiation · Osteoimmunology · Bone repair · Osteoporosis

Introduction

Osteoporosis is a kind of chronic systemic bone disease which is characterized with low bone mass, bone microstructure destruction, fragility of bone, and susceptibility to fracture [1]. Low bone mass may cause functions on supporting, protection and resistance damaged. The change of bone mass is primarily influenced by bone metabolism, whose steady state is maintained through the balance between bone formation and resorption [2]. Normally, skeletons are ceaselessly formed, absorbed and shaped. Bone formation is mainly accomplished by osteoblasts that are differentiated from bone marrow mesenchymal stem cells (BMSCs) and secrete a large amount of collagen and extracellular matrix that gradually transform into bone tissue as calcium deposits [3]. Before adulthood, there existing a positive balance between bone formation and resorption that leads to growth of bone mass, which ultimately climbing to the summit. After reaching adulthood, bone metabolism keeps balance, maintaining bone mass steady. However, under aging or pathological conditions, such as autoimmune diseases,

bone resorption by osteoclasts exceeds bone formation by osteoblasts, which causes chronic loss of bone mass, giving rise to osteopenia and osteoporosis [4, 5]. Previous published papers demonstrates the reason why this phenomenon occurs is that osteogenic differentiation potential of BMSCs decreases. As one grows older, proliferation and differentiation ability of BMSCs towards osteoblasts constantly declines, and the signal promoting osteogenesis of osteogenic precursor cells decreases as well, which leads to reduction of osteoblasts [6, 7]. However, the specific mechanism underlying the decay in osteogenic differentiation potential of BMSCs has not been elucidated yet.

Transcriptome sequencing, namely RNA sequencing (RNA-seq), is a revolutionary biological technology that emerged in the 2010 s. Because of the capability to provide a precise measurement of level of transcripts, RNA-seq has been widely utilized to explore molecular mechanism of osteogenesis [8–10]. In this study, we analyzed bulk transcriptome and single-cell sequencing data downloaded from public databases and found that FKBP5 was upregulated during osteogenesis of MSCs. FK506-Binding Protein

5 (FKBP5) is a protein-coding gene, whose coded protein primarily exists in the nucleus, cytoplasm, and extracellular space. This gene is involved in the trigger and development of inflammation-related diseases. For example, under the condition of aging and stress, the epigenetic upregulation of FKBP5 can promote the occurrence of NF- κ B-driven inflammation and increase the risk of cardiovascular disease [11]. Our function tests confirmed that FKBP5 exerted an important impact on osteogenic process. RNA-seq suggested that FKBP5 inhibited the expression of genes in the type-I interferon (IFN)-related pathway. In recent years, this pathway has been shown to inhibit osteogenic differentiation in mice [12]. We successfully verified through a series of experiments that the type-I IFN pathway affects osteogenic differentiation of BMSCs and that FKBP5 regulates osteogenic differentiation of BMSCs through this pathway. We systematically analyzed the core molecule involved in the differentiation of BMSCs into osteoblasts and elucidated the mechanism by which FKBP5 regulated the osteogenesis of BMSCs. We believe that our research provides a potential gene target and theoretical basis for diseases where bone formation serves as a therapeutic approach.

Materials and methods

Bioinformatics analysis

For bulk RNA-seq analysis, public datasets (GSE178679, GSE183931, and GSE80614) were acquired from the Gene Expression Omnibus (GEO) database (<https://www.ncbi.nlm.nih.gov/geo/>), which included RNA-seq or microarray data before and after osteogenic induction of human BMSCs. Rtool and R studio software (version 4.4.1) were used to analyze the differentially expressed genes before and after osteogenic induction with filter criteria of $|\log_{2}FC| > 2$ and $\text{adj.P.Value} < 0.05$ using the R package “limma”. The R language used in this study is adapted based on the code provided by the GEO database. For single cell sequencing (scRNA-seq) analysis, we downloaded data of GSE147390 from GEO database as well. This dataset includes samples of preosteoblast (preOB) and mature osteoblast (matOB). We filtered the individual cells, requiring that the number of genes detected in each cell be greater than 800, the fraction of mitochondrial transcripts be less than 20% and UMI > 100 . The remaining 7615 cells were used for subsequent cluster annotation and analysis. Due to their high expression in BMSCs, in this article, we considered ITGB1 and ENG as marker genes for preOBs, while IBSP, BGLAP, and SPP1 were regarded as marker genes for matOB.

Cell isolation and culture

BMSCs were purified and isolated by employing the methods we had previously reported [13, 14]. Bone marrow was extracted from the lumbar vertebrae and mixed with separation solution (6% hydroxyethyl starch plus 0.9% sodium chloride). The mixture was allowed to stand for approximately 20 min, and then the supernatant was collected and centrifuged at $2000 \times g$ for 20 min. Subsequently, BMSCs were collected and cultured in complete medium composed of low-glucose medium (DMEM, Gibco, USA) and 10% fetal bovine serum (FBS, Zhejiang Tianhang Biotechnology, China). Three days later, the detached cells were removed by replacing half of the medium. After that, the culture medium was completely replaced every 3 days. When the BMSCs reached 80–90% confluence, they were digested with trypsin and divided into two new culture flasks. After 1 to 2 passages, under the microscope, it could be observed that there were no residual contaminating cells (such as monocytes and dendritic cells), and only long spindle-shaped mesenchymal stem cells remained. The BMSCs used in this study were at passage 2–4. BMSCs at a density of 1×10^5 or 15×10^5 cells per well were seeded in 24 or 6-well plates for osteogenic induction and further experiments.

Multipotent differentiation potential of BMSCs

The stemness of BMSCs can be assessed by testing their trilineage differentiation potential (osteogenic, adipogenic, and chondrogenic). For osteogenic induction, the osteogenic differentiation medium (OM) was composed of 10% fetal bovine serum (FBS) in low-glucose DMEM, 100 IU/ml penicillin-streptomycin (Beyotime, China), 0.1 μ M dexamethasone (APEX BIO Technology, USA), 10 mM β -glycerophosphate (APEX BIO Technology, USA), and 50 μ M ascorbic acid (APEX BIO Technology, USA). For six-well plates, 2 ml of OM was added to each well, while for 24-well plates, 0.5 ml of OM was used per well. The OM was replaced every 3 days until BMSCs were ready for subsequent assays.

For adipogenic induction, BMSCs were seeded into 24-well plates at the aforementioned density. The adipogenic induction medium consisted of DMEM supplemented with 10% FBS, 100 IU/ml penicillin-streptomycin (Beyotime, China), 0.5 mM 3-isobutyl-1-methylxanthine (Sigma-Aldrich, USA), 1 mM dexamethasone (APEX BIO Technology, USA), 10 mg/ml insulin (Sigma-Aldrich, USA) and 0.2 mM indomethacin (Sigma-Aldrich, USA). The medium was replaced every three days, and Oil Red O (ORO) staining was performed on the 14 th day of induction.

When conducting chondrogenic induction, the serum-free chondrogenic medium was composed of high-glucose

DMEM, 1% ITS Premix (Corning Life Sciences, USA), 50 mg/l ascorbic acid (APEX BIO Technology, USA), 1 mM sodium pyruvate (Sigma-Aldrich, USA), 100 nM dexamethasone (APEX BIO Technology, USA), and 10 ng/ml recombinant human TGF- β 3 (R&D Systems, USA). Toluidine blue staining could be performed on the 21 st day of induction.

ALP and ARS staining assay

BMSCs were fixed with 4% paraformaldehyde for 20 min and then washed with phosphate-buffered saline (PBS) solution. Staining solution was prepared according to instruction of BCIP/NBT ALP kit (Beyotime, China) and was added to wells. Subsequently, the plate was incubated in dark for 20 to 30 min before being photographed under microscope. For alkaline phosphate (ALP) activity assessment, BMSCs after osteogenic induction were lysed with RIPA buffer. The protein concentration was measured by using BCA Protein Assay Kit (Beyotime, China), and absorbance was determined with ALP activity detection kit (Beyotime, China) using spectrophotometer. These two values were used together to calculate ALP activity.

BMSCs were fixed as forementioned methods and dyed with 1% Alizarin Red S (ARS) for 20 min. After discarding the solution, the cells were washed with PBS solution three times. After mineralized nodules were observed and captured under microscope, cetylpyridinium chloride monohydrate solution (Sigma-Aldrich) was added to plate wells to dissolved mineralized nodules, and then absorbance was measured at a wavelength of 562 nanometers using spectrophotometer.

RNA interference

The small interfering RNAs (siRNAs) targeting FKBP5 and IFIT2 were purchased from GenePharma (Suzhou, China). When the seeded BMSCs reached 70–90% confluence, transfection was performed using the jetPRIME kit (Niuqi Health, China) according to instruction.

Cell viability assay

A CCK8 assay was utilized to assess cell viability of BMSCs after transfection. According to the instruction of manufacturer (APEX BIO Technology, USA), BMSCs were seeded into 96-well plates containing complete culture medium for 24 h with density of 5×10^3 cells per well. Following this, BMSCs were transfected with siRNA or lentivirus, with the detailed transfection protocol described elsewhere in the methods section. 24 h after the transfection experiment, the culture medium in the 96-well plate was aspirated

completely. Each well was then replenished with 90 μ l of fresh medium and 10 μ l of CCK-8 solution. The plate was incubated in a humidified environment of 95% air and 5% CO₂ for 1.5 h at 37 °C. Subsequently, the absorbance of each well at 450 nm was measured using a microplate reader. The cell viability was presented as a percentage relative to the control.

Total RNA extraction and qPCR

The EZ-press RNA Purification Kit (EZBioscience, USA) was utilized for extraction of total RNA. Subsequently, reverse transcription was performed using the Evo M-MLV III Reverse Transcriptase Kit (Accurate Biology, China), where the resulting cDNA from mRNA served as the template for amplification with the Evo M-MLV One-Step RT-qPCR Kit (Accurate Biology, China). Following the manufacturer's instruction, RT-qPCR were conducted employing commercially available forward primers and reverse primers (Gene Create, China). Relative expression was evaluated by normalizing against the expression of GAPDH. The primer sequences used are presented in Table S1.

Western blot

Culture medium in six-well plate was discarded and BMSCs were washed with PBS. RIPA buffer mixed with phosphatase inhibitor and protease inhibitor (1:100) was added to the plate. The plate was then left to stand on ice for 25–30 min. The cell lysate was aspirated and centrifuged at 14,000 g for 15 min to precipitate the organelles. Then the supernatant was collected and mixed with loading buffer at a ratio of 4:1. 10 μ l of protein was added to each lane of the gel in equal amounts. After electrophoresis completed, the protein was transferred from gel to a 0.45 μ m polyvinylidene difluoride (PVDF) membrane. The membrane was blocked with 5% non-fat milk for 1 h and then incubated with the specified primary antibody overnight at 4°C. Subsequently, the membrane was washed employing Tris Buffered Saline Tween (TBST) for 5 min each time for three times. Secondary rabbit or mouse antibody was utilized to incubated the membrane.

The antibodies used for western blot to detect protein were as follows: anti-FKBP5 (Proteintech, 14155-1-AP, 1:1000); anti-IFIT2 (Proteintech, 12604-1-AP, 1:1000); anti-RUNX2 (Proteintech, 20700-1-AP, 1:1000); anti-Collagen I (Coll; Proteintech, 67288-1-Ig, 1:1000); anti-GAPDH (Proteintech, 60004-1-Ig, 1:5000); and HRP-conjugated secondary antibodies (ABclonal, 1:5000).

Bone formation assay in vivo

Full-length overexpression and knockout lentivirus of FKBP5 for human, and full-length overexpression lentivirus of FKBP5 for mouse were purchased from Hanyi Biotechnology in Wuhan, China. These viruses were constructed on GFP-loaded lentiviral vectors. When transfecting BMSCs, the lentivirus dosage was calculated at a multiplicity of infection (MOI) of 10, and transfection-enhancing reagent (1:1000) was mixed into culture medium simultaneously. 24 h later, the medium was replaced with fresh medium. A part of cells was applied to perform western blot to verify overexpression and knockdown efficiency. The remaining cells were absorbed onto hydroxyapatite scaffold that was implanted into subcutaneous tissue of nude mice.

Tibial defect repair experiment

8-week-old C57 mice were anesthetized with 1% pentobarbital sodium. A small incision was made on tibial skin. Muscle tissue was separated, and bone surface was exposed. A hole was perforated using drilling machine with a 0.6-mm sterilized head. Later, FKBP5 overexpression lentivirus was injected into the hole with Hamilton syringe. The wound was sutured afterwards, and mouse tibiae were acquired for micro-CT scan and section after one week.

Section staining

Before staining, sections were initially dewaxed with xylene and then hydrated with ethanol. For hematoxylin&eosin (H&E) staining, the kit was from Solarbio (China). According to the direction, the sections were dyed in hematoxylin for 1 min, washed with 70% alcohol containing 1% HCl for 5 s and stained with eosin for 1 min. Masson staining was performed in the light of Masson's trichrome staining kit (Solarbio, China). Following the instruction provided in the immunohistochemistry (IHC) kit (CW BIO, China), IHC stain was conducted adopting FKBP5 (Proteintech, 14155-1-AP, 1:100) and RUNX2 (Proteintech, 20700-1-AP, 1:100) antibodies.

Statistical analyses

The experiments were performed independently three times. Results of this study were analyzed by using GraphPad Prism 9.0. Correlation analysis was conducted employing Pearson correlation and linear regression. Difference between diverse groups was evaluated using student t-tests or one-way ANOVA. $P < 0.05$ was regarded as significant. The result value was presented in form of mean \pm SEM (standard error of the mean).

Results

FKBP5 expression is up-regulated during osteogenic differentiation of BMSCs and down-regulated in osteoporotic bone

We carried out differential gene analysis using three public datasets (GSE178679, GSE183931, and GSE80614), whose results revealed significant alteration in gene expression profile of BMSCs after osteogenic induction compared to pre-induction (Fig. 1A). By screening genes with significant expression changes, we identified 18 consistently upregulated key genes across all three independent datasets (Fig. 1B and Table S2), including CIDEA, FKBP5, CFD, SAA1, LEP, TSC22D3, IGFBP2, ZBTB16, SORT1, SUSD2, IGF2, FMO3, TIMP4, APOD, AOX1, FOXO1, NPR3, and PPARG. Notably, FKBP5 exhibited relatively higher expression level and statistical significance than most others. For this reason, we attempted to conduct theoretical and experimental verification. First in the place, bioinformatic analysis of scRNA-seq dataset, GSE147390, was performed. When running cluster annotation, ITGB1 and ENG that generally were deemed to be markers for BMSCs were regarded as signs of incomplete differentiation into matOB in the present study. IBSP, BGLAP, and SPP1 were utilized as markers of matOB. We found that FKBP5 exhibited higher expression level among matOB than that of preOB (Fig. 1C). Now that relatively high expression of FKBP5 during osteogenesis was hinted in theoretical analysis, experimental confirmation was naturally arranged. Bone samples were obtained from patients with osteoporosis and intervertebral disc herniation during discectomy and from ones with spine fracture during vertebral fixation. H&E staining showed denser and thicker bone trabeculae of normal bone (NB) compared to that of osteoporotic bone (OB). IHC showed that range and intensity of both RUNX2 and FKBP5 staining were at higher level in NB, indicating superior expression of RUNX2 and FKBP5 in healthy persons (Fig. 1D). To further elucidate the expression dynamics of FKBP5 during osteogenic differentiation in human BMSCs, we subjected BMSCs to time-course osteogenic induction. RT-qPCR results showed that the expression of FKBP5 increased with prolonged induction time and peaked on the 7th day. In addition, there was a positive correlation between FKBP5 and RUNX2 mRNA (Fig. 1E). Western blot also presented expression trend of FKBP5 protein similar to RT-qPCR (Fig. 1F). These results suggested that FKBP5 might play a critical role in osteogenic differentiation of BMSCs, and for this reason, FKBP5 was selected for further research.

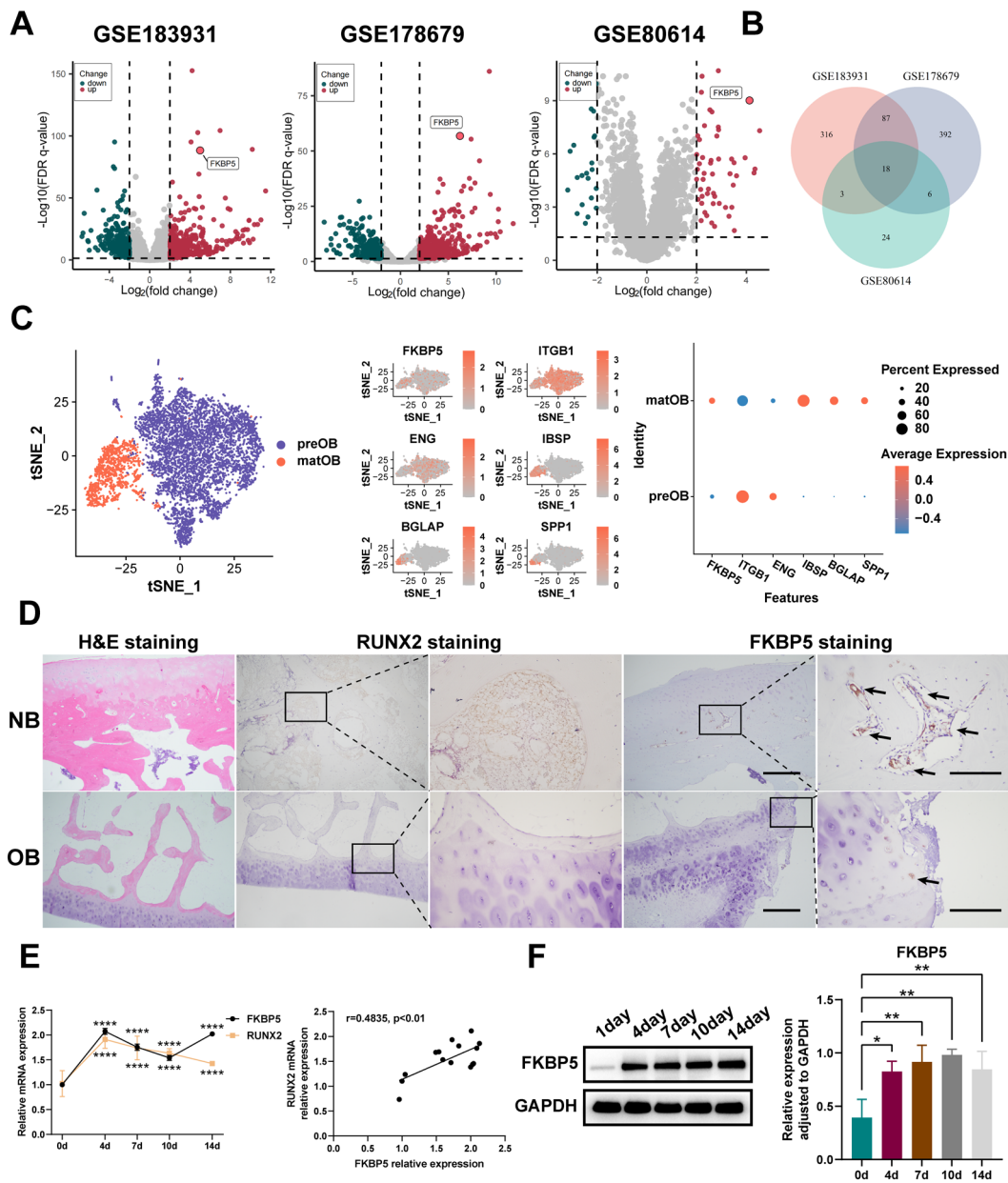


Fig. 1 FKBP5 is up-regulated during the osteogenic differentiation of BMSCs and down-regulated in osteoporotic bone. **A** The volcano plots of the RNA-seq datasets (GSE178679, GSE183931 and GSE80614) from the GEO database displayed the differentially expressed genes in BMSCs after osteogenic induction. **B** The Venn diagram showed the commonly upregulated genes across three public datasets. **C** The analysis result of the single-cell dataset (GSE147390) indicated that FKBP5 was expressed at a higher level in matOB. **D** The bone trabeculae of NB were significantly denser and thicker than those of cancel-

ous bone. IHC staining showed both RUNX2 and FKBP5 were highly expressed in normal bone (left scale bar: 200 μm , right scale bar: 50 μm). **E** RT-qPCR showed mRNA of both FKBP5 and RUNX2 were significantly up-regulated during osteogenic induction of BMSCs, and the expression level of these two genes were positively correlated. **F** Western blot demonstrated FKBP5 protein in BMSCs significantly increased after osteogenic induction. All experiments were performed three independent times

FKBP5 promotes osteogenic differentiation of BMSCs in vitro

In order to investigate osteogenesis regulation function of FKBP5, we firstly silenced FKBP5 using siRNA. The CKK8 assay revealed that the two FKBP5 siRNAs did not reduce the viability of BMSCs (Fig. 2A). Downregulation of FKBP5 resulted in decreased mineralized nodule formation and ALP staining intensity (Fig. 2B), accompanied by corresponding decline in ARS quantification and ALP activity (Fig. 2C). Besides, western blot images also showed lower protein level of osteogenic markers (RUNX2 and COL1 A1) after addressing with siRNA targeting FKBP5 (Fig. 2D). Further overexpression of FKBP5 through transfecting lentivirus did not obviously affect BMSC viability and made the opposite staining and protein tendency (Fig. 2E and H). All in all, these results indicated that FKBP5 positively regulated the osteogenic differentiation of BMSCs in vitro.

FKBP5 promotes osteogenesis of BMSCs in vivo

Previous experiments have shown that FKBP5 could promote osteogenic differentiation of BMSCs under in vitro condition, but it was still unknown whether this effect held true under in vivo condition. For the sake of elucidate this question, experiment of porous hydroxyapatite scaffold implantation into subcutaneous tissue of nude mice was carried out. We supplemented the cell viability experiment using knockdown lentivirus of human FKBP5. Statistically, the results indicated that transfecting BMSCs with FKBP5 knockdown lentivirus did not significantly reduce cell viability (Fig. 3A). The results of the cell viability experiment using overexpression lentivirus of human FKBP5 are shown in Fig. 2E. As illustrated in Fig. 3B, we firstly transfected BMSCs with negative control lentivirus for knockdown (shNC), FKBP5 knockdown lentivirus (shFKBP5), negative control lentivirus for overexpression (ovNC), and FKBP5 overexpression lentivirus (ovFKBP5). These cells were cultured in osteogenesis induction medium for 7 days. Following this, they were transferred and adsorbed onto hydroxyapatite scaffold that was then implanted into subcutaneous tissue of nude mice. 8 weeks later, the nude mice were sacrificed, and granulation tissue containing hydroxyapatite scaffold was acquired and sectioned for staining. H&E staining revealed that in contrast to ovNC group, overexpression group showed more new bone formation, while shFKBP5 group showed less formation compared to shNC group (Fig. 3C). Similar to the result of H&E, Masson staining showed more collagen formation in ovFKBP5 group and less in shFKBP5 group (Fig. 3D). IHC staining for detecting RUNX2 demonstrated more extensive positive area in ovFKBP5 group compared to ovNC group, while shFKBP5

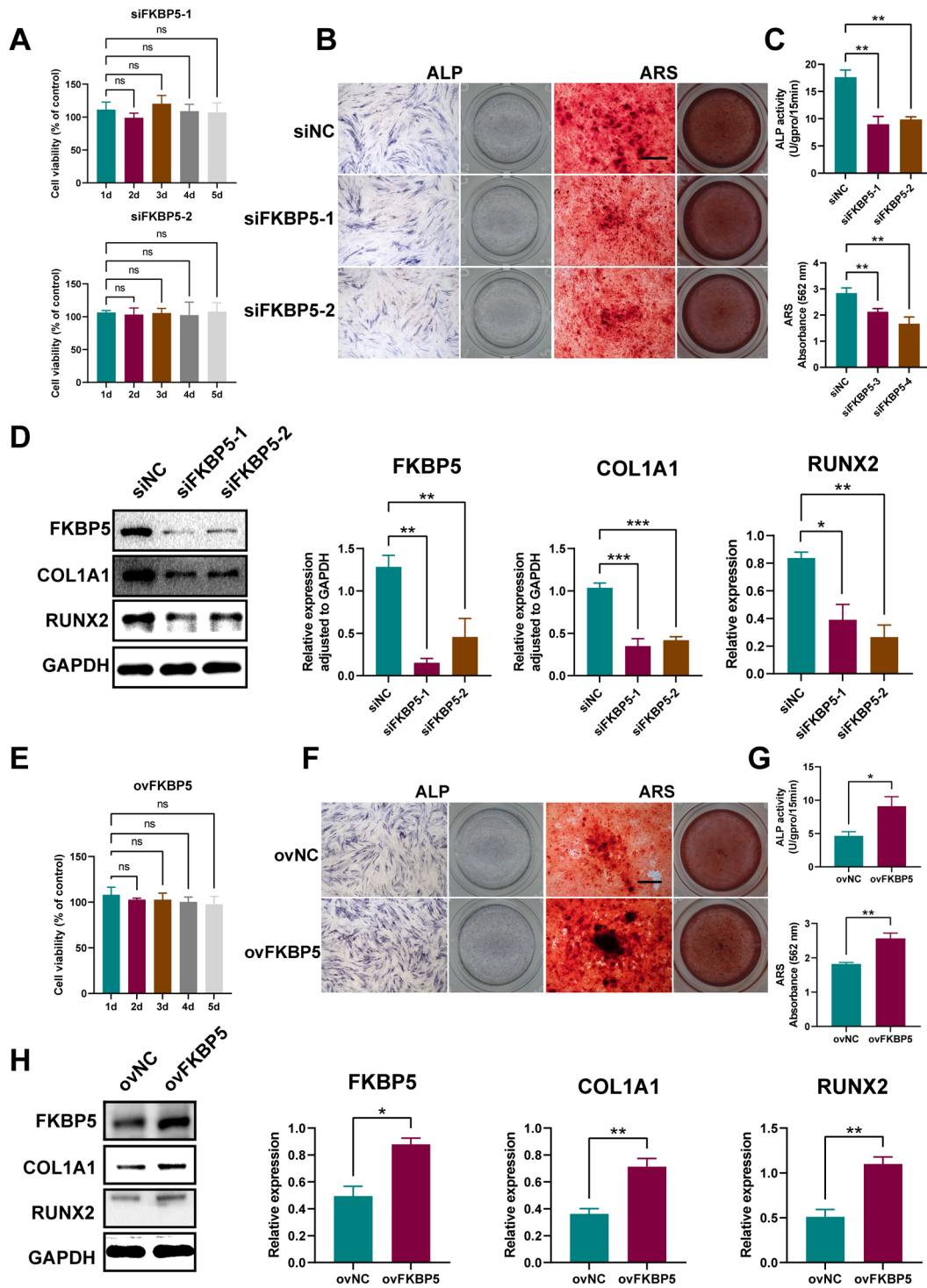
and shNC group showed an opposite trend (Fig. 3E). The difference in positive area of IHC staining was statistically significant (Fig. 3F). In conclusion, these results displayed obvious osteogenic-promoting effect of FKBP5 on BMSCs in vivo.

RNA-seq indicates type-I IFN pathway is up-regulated after silencing FKBP5

In order to explore the mechanism that FKBP5 regulated osteogenic differentiation, we transfected BMSCs with siRNA targeting FKBP5 and collected the cells for RNA-seq. The result showed that gene expression profile of siFKBP5 group significantly changed compared to siNC group (Fig. 4A). We extracted up-regulated genes in siFKBP5 group and performed a series of enrichment analysis. Reactome pathway analysis suggested elevated genes markedly enriched in the interferon (IFN) alpha/beta signaling pathway, also known as type-I IFN pathway (Fig. 4B). Furthermore, biological processes of gene ontology (GO) enrichment analysis showed expression of genes in type-I interferon signaling pathway increased (Fig. 4C). Gene Set Enrichment Analysis (GSEA) enrichment analysis revealed similar result (Fig. 4D, E). The specific up-regulated genes in this pathway consisted of IFIT2, ISG15, ISG20, RSAD2, IRF4, IRF5, IRF7, and IFITM1 (Fig. 4F). Given there existing published articles suggesting type-I IFN pathway played a vital role in regulating osteogenic differentiation [12, 15], we hypothesized that it serves as a downstream pathway for FKBP5 to modulate osteogenic differentiation of BMSCs.

FKBP5 mitigates the osteogenic inhibitory effect of IFN β

Previous RNA-seq analysis showed genes, including multiple interferon-stimulated genes (ISG), namely IFIT2 (ISG54), ISG15, ISG20, and IRF7, in type-I IFN signaling pathway were significantly up-regulated as a result of FKBP5 knockdown, which implied that FKBP5 might influence osteogenesis of BMSCs through regulating this pathway. We validated the changed ISG identified by the RNA-seq via using RT-qPCR. Consistent with theoretical alteration, IFIT2, ISG15, ISG20 and IRF7 were significantly up- or down-regulated when FKBP5 was knocked down or overexpressed (Fig. 5A). Furthermore, RT-qPCR showed that exogenous IFN β induced up-regulation of ISG in BMSCs (Fig. 5B). IFN β exerted obviously repression effect on osteogenesis of BMSCs in a dose-dependent way, which manifested as lighter ALP staining and reduced mineralized nodule formation (Fig. 5C). The quantitative analysis of mineralized nodules and ALP activity showed the trend was statistically significant (Fig. 5D). Downregulation of ISG



when FKBP5 was overexpressed demonstrated that FKBP5 might be able to suppress the effect of IFN β on BMSCs. As expected, compared to IFN β -treated group, the group overexpressing FKBP5 and treated with IFN β has deeper ALP staining and more mineralized nodule formation (Fig. 5E).

Quantification indicated a statistically significant difference among the three groups (Fig. 5F). Western blot experiment also confirmed that protein expression of RUNX2 and COL1 A1 of FKBP5 overexpression plus IFN β group was effectively up-regulated in contrast to IFN β -treated group

Fig. 2 FKBP5 positively regulates the osteogenesis of BMSCs. The expression of FKBP5 can be downregulated using siRNAs, while overexpression can be achieved through lentiviral transduction. **A** Cell viability assessment of BMSCs transfected with siFKBP5. **B** siRNAs targeting FKBP5 significantly reduced the intensity of ALP and ARS staining of BMSCs (scale bar: 200 μ m). **C** Quantitative analysis indicated that downregulation of ARS staining and ALP activity by employing FKBP5 siRNA was statistically significant. **D** siRNAs targeting FKBP5 successfully reduced the protein expression of FKBP5, RUNX2, and Col1 A1 in BMSCs. **E** Cell viability assessment of BMSCs transfected with FKBP5 overexpression lentivirus. **F** FKBP5 overexpression significantly increased ALP and ARS staining of BMSCs (scale bar: 200 μ m). **G** Quantitative analysis indicated that the upregulation of ARS and ALP activity by transfecting lentivirus was statistically significant. **H** FKBP5 overexpression successfully up-regulated the protein level of FKBP5, RUNX2, and Col1 A1 in BMSCs. All experiments were performed three independent times

(Fig. 5G). In summary, previous literatures have shown that activation of the type-I interferon signaling pathway could result in osteogenic impairment, and FKBP5 was able to inhibit this effect.

FKBP5 promotes osteogenic differentiation by inhibiting IFIT2 expression

Since IFIT2 was a well-documented member of ISG family and was proved to inhibit osteogenic differentiation of human stem cells from apical papilla (hSCAPs) [15], we thought IFIT2 might be able to exhibit analogous effect on osteogenesis of human BMSCs. Therefore, we chose this gene as a crucial downstream molecule for further mechanism research.

Inconsistent with expectation, RT-qPCR suggested that expression level of IFIT2 increased with the time progress of osteogenic induction, which reached peak on the 7th day (Fig. 6A). The result of western blot was consistent with RT-qPCR (Fig. 6B). Then, we verified protein expression of IFIT2 when FKBP5 was knocked down and overexpressed. In accord with previous result of RT-qPCR, IFIT2 protein increased when FKBP5 was inhibited and decreased when FKBP5 was overexpressed (Fig. 6C). In order to evaluate the impact of the IFIT2 gene on the osteogenic differentiation of BMSCs, we transfected BMSCs with siRNA to reduce the intracellular expression of IFIT2 and subsequently assessed the effect of siIFIT2 on cell viability. The results demonstrated that, compared to the control group, there was no statistically significant decrease in the cell viability of BMSCs transfected with siIFIT2 (Fig. 6D). ARS and ALP staining results suggested that silencing IFIT2 through siRNA resulted in enhanced osteogenesis of BMSCs (Fig. 6E). The difference of mineralized nodules and ALP activity between siNC and siIFIT2 groups was statistically significant

(Fig. 6F). Western blot showed corresponding higher protein level of RUNX2 and COL1 A1 (Fig. 6G).

To confirm that FKBP5 affected the osteogenic differentiation of BMSCs by regulating the expression of IFIT2, we established three cell experimental groups: siNC, siFKBP5, and siFKBP5 + siIFIT2. The results indicated that IFIT2 silence could relieve reduced ALP and ARS staining caused by FKBP5 down-regulation, whose significance was determined by quantitative assessment (Fig. 6H and I). Correspondingly, western blot showed that when FKBP5 was knocked down, IFIT2 expression was upregulated, and protein level of RUNX2 and COL1 A1 was correspondingly downregulated. However, when IFIT2 was further knocked down simultaneously, the protein expression of these two osteogenic markers did not significantly decrease (Fig. 6J). In summary, these results suggested that IFIT2 had an inhibitory effect on osteogenesis of BMSCs, and FKBP5 exerted influence on osteogenic differentiation of BMSCs through regulating this gene.

FKBP5 overexpression accelerates bone defect repair in vivo

In previous experiment of porous hydroxyapatite scaffold implantation, we confirmed FKBP5 promoted osteogenesis of BMSCs in vivo. However, it has not been known whether FKBP5 was able to accelerate bone healing. We decided to clear this question by establishing mouse tibial drilling model.

The anesthesia and surgical process of C57 mice were performed as described in METHODS section and was illustrated in Fig. 7A, B. The C57 mice were sacrificed one week after surgery, and tibiae were acquired to perform micro-CT scan and decalcification. Images of micro-CT showed more amount of visible callus formation in drilling site of tibia of ovFKBP5 group than ovNC group at the same window width and window level (Fig. 7C). Quantitative analysis suggested the same result (Fig. 7D). As shown via H&E staining and SO/FG staining in Fig. 7E and F, more portion of bony callus formed in ovFKBP5 group, while ovNC group showed less, indicating that tibia trauma of ovFKBP5 group were in formation stage of bony callus and that bone remodeling of ovNC group lagged behind that of ovFKBP5 group. IHC analysis also illustrated up-regulation of RUNX2 expression in healing sites of tibia in ovFKBP5 group (Fig. 7G). In conclusion, this experiment demonstrated that FKBP5 overexpression significantly accelerated the process of bone healing.

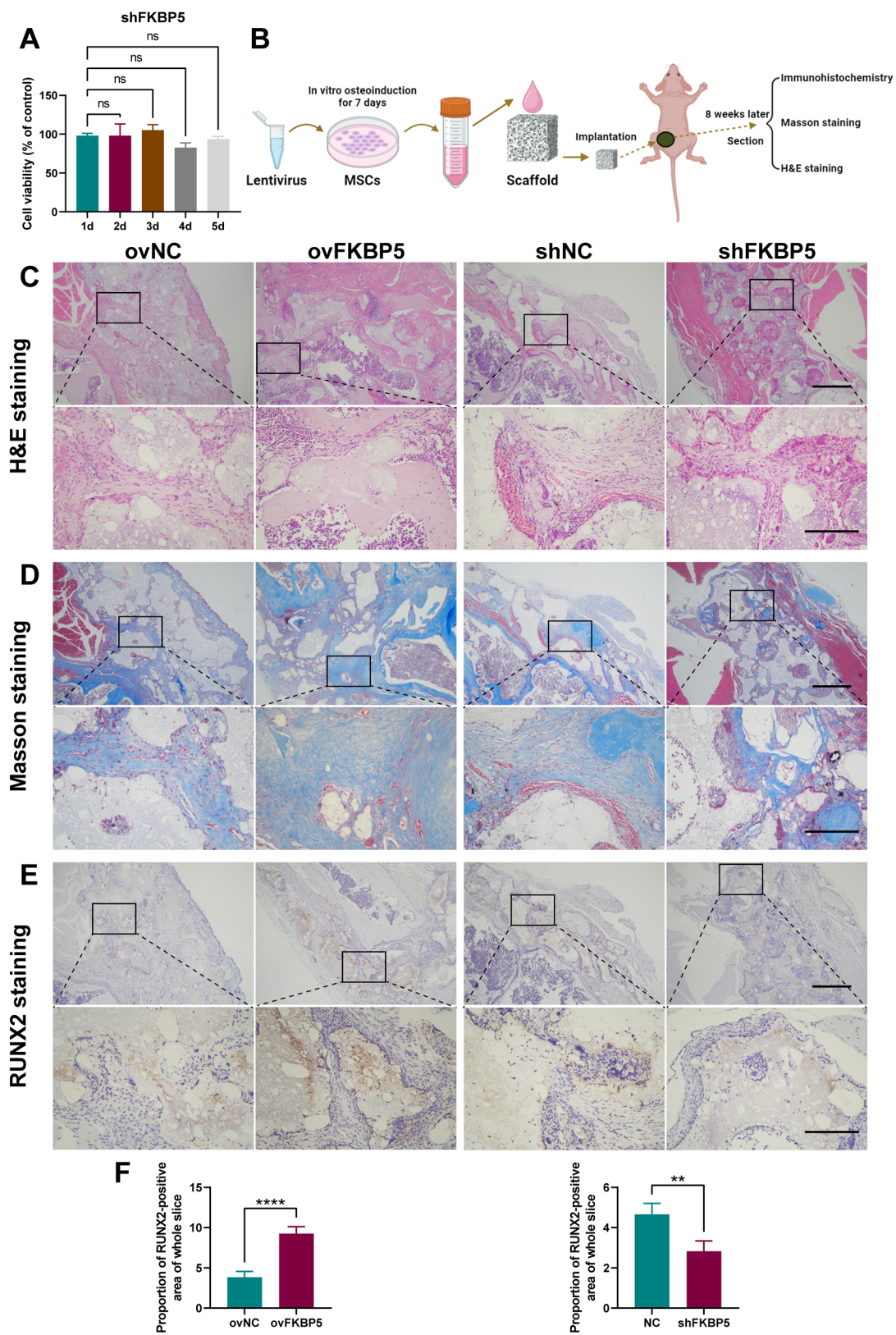


Fig. 3 FKBP5 promotes osteogenic differentiation of BMSCs in vivo. **A** Cell viability assessment of BMSCs transfected with FKBP5 knock-down lentivirus. **B** Following transfecting BMSCs with lentivirus, osteogenic induction was performed for 7 days in vitro. Then these cells were transferred onto porous hydroxyapatite scaffold, which was implanted into subcutaneous tissue of nude mice. 8 weeks later, the scaffold was taken out, sectioned, and stained. **C** H&E staining showed more new bone formation in the ovFKBP5 group, while there was less in the shFKBP5 group (upper scale bar: 200 μ m, lower scale bar: 50 μ m). **D** Masson staining revealed increased collagen formation in the ovFKBP5 group, whereas collagen decreased in the FKBP5-knockdown group (upper scale bar: 200 μ m, lower scale bar: 50 μ m). **E** IHC staining demonstrated wider positive range of RUNX2 in the ovFKBP5 group compared to shFKBP5 group (upper scale bar: 200 μ m, lower scale bar: 50 μ m). **F** The differences of positive area of RUNX2 between ovNC and ovFKBP5 and between shNC and shFKBP5 were statistically significant. All experiments were performed independently and repeated three times, $n = 5$

Discussion

In the present research, we identified a key protein, FKBP5, whose expression level increased during osteogenic induction and accelerated the osteogenesis of BMSCs. Mechanistically, FKBP5 suppressed type-I IFN signaling and relieved negative osteogenic effect of IFN β . Moreover, the enhanced level of FKBP5 reduced the transcription of IFIT2 which was considered as an inhibitory gene for osteogenic differentiation. Furthermore, we found that FKBP5 over-expression improved tibial defect repair in vivo. A recent study revealed that FKBP5 enhances the osteogenic differentiation of human adipose-derived stem cells (ASCs) [16]. Although this study did not include in vivo experiments for verification and ASCs differ from BMSCs in tissue origin, their findings still support our experimental conclusions to a certain extent.

Normal osteogenic activity that is mainly executed by osteoblasts is a necessary premise for maintaining bone homeostasis [17]. Deviant osteogenesis may cause diverse bone diseases, such as osteoporosis or delayed bone healing [18, 19]. In other words, when bone loss caused by aging process or auto-immune disease occurs, MSCs' commitment towards the osteogenic lineage is always impaired [20]. As BMSCs are the main source of osteoblasts, effective correction of the differentiation of BMSCs into osteoblasts can alleviate or even reverse bone loss. Hence, exploration of the regulatory network of osteogenic differentiation of BMSCs from different perspectives appears to be crucial.

Osteoimmunology that focuses on the interaction between the immune system and bone metabolism has received increasing attention. With the deepening of the research on the bone homeostasis, it has been confirmed that low-grade inflammation is involved in bone loss during aging process and auto-immune diseases. Multiple cytokines produced by immune cells, commonly including TNF, IL-1, IL-6, IL-17, IL-22, IFN γ are reported to play crucial roles in

bone formation and resorption [21–24]. The incidence that patients with systemic lupus erythematosus (SLE) suffer from osteoporosis is as high as 5–20% which exceeds that of healthy individuals in the same age group (15–44 years old), implying there is a certain immune factor contributing to bone loss [25]. Nevertheless, despite the significance of type-I IFNs in promoting pathogenesis and treatment of auto-immune diseases such as SLE [26], their role in osteoimmunology has not received sufficient attention and research. Type-I IFNs, including IFN α , IFN β , IFN ω , IFN ϵ and IFN κ , are well-known key drivers of chronic inflammation of SLE [27, 28]. Among these factors, IFN β plays roles in amplifying DNA damage, promoting senescence and inhibiting function of stem cells. It is definitely confirmed to be produced by BMSCs, and the quantity increased in BMSCs derived from patients with SLE [27, 29]. In our study and previous published papers, IFN β significantly weakens osteogenesis, matrix formation and mineralization [27, 30, 31]. Because of this effect, BMSCs produce IFN β through autocrine during osteogenic induction, which in turn inhibits osteogenesis and enhanced the ISG expression [12]. This phenomenon partially explains why IFIT2, as an inhibitory gene of osteogenesis, shows increased expression during osteogenic induction of BMSCs. It also reflects the potential existence of negative feedback in the osteogenesis process of human BMSCs, where auto-secreted IFN β activates type-I IFN pathway and inhibits osteogenesis. Knock-down of FKBP5 may result in excessive activation of this negative feedback, causing tardiness of osteogenic process. Combining these clues, blocking IFN β pathway might be a research direction of potential application value. FKBP5 inhibits ISG expression and rescues IFN β -induced delayed osteogenesis, indicating that FKBP5 plays a blocking role in the feedback to some extent.

IFIT gene family is clustered on human chromosome 10 and composed of four members: IFIT1, IFIT2, IFIT3, and IFIT5, among which IFIT2 is also known as ISG54 because of its molecular weight of 54 kDa [32]. This molecule is linked to diverse immune system diseases. The expression level of IFIT2 in peripheral white blood cells of SLE patients is significantly higher than that of non-SLE patients and normal control group. Furthermore, the real-time expression level of the IFIT2 gene is correlated with the disease activity of SLE [33]. This characteristic makes IFIT2 a potential new target for SLE treatment. Since type-I IFN is a key driver of chronic inflammation in SLE, and IFIT2 has inhibitory function to osteogenic differentiation, it is possible that bone loss of SLE patients may also be partially caused by up-regulation of this gene. However, this assumption needs to be authenticated in the future research.

It is worth noting that IFIT2 is not the only ISG reported to have inhibitory effects on osteogenic differentiation.

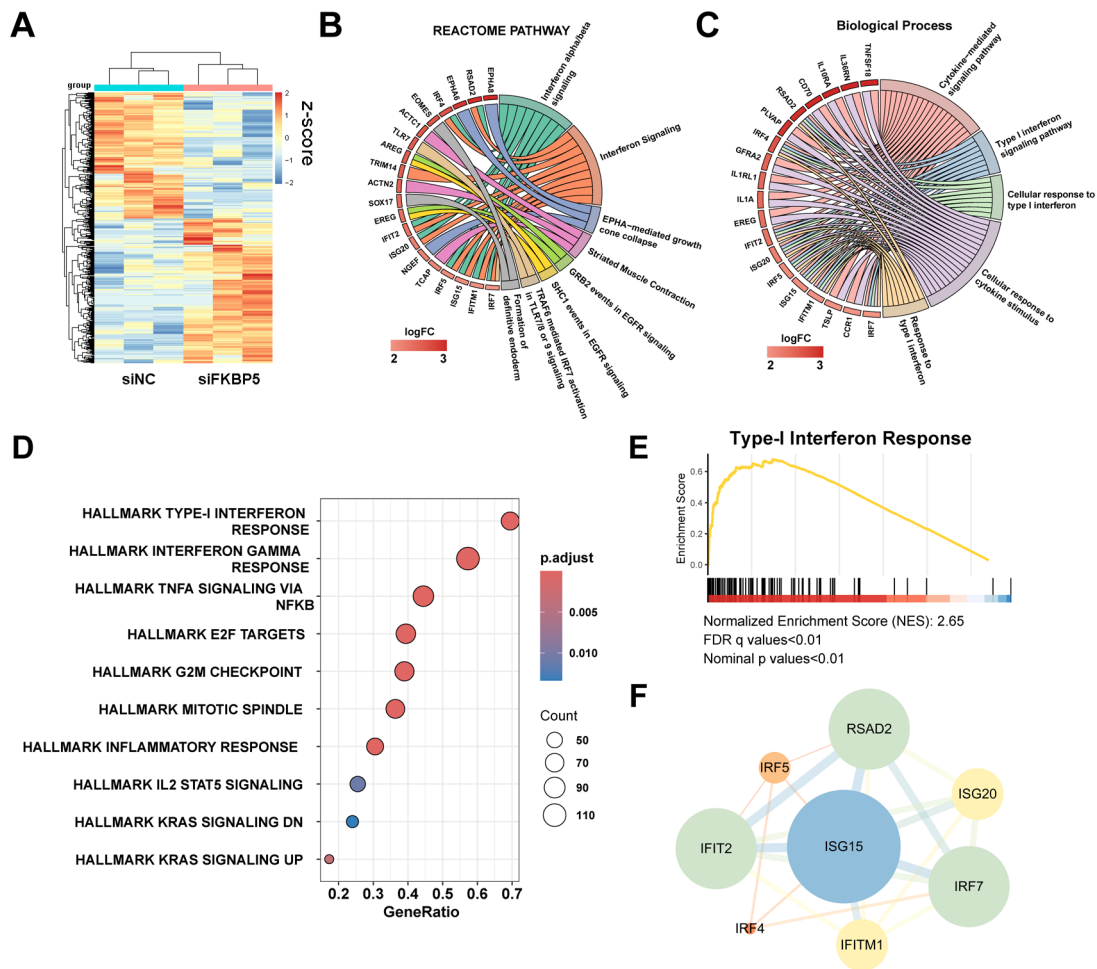


Fig. 4 Knockdown of FKBP5 up-regulates type-I interferon signaling pathway and ISG expression. **A** The heatmap of RNA-seq showed differentially expressed genes of BMSCs after FKBP5 knockdown. **B** Reactome enrichment revealed that some of the up-regulated genes identified through RNA-seq analysis were enriched in the interferon alpha/beta signaling pathway, also known as type-I IFN signaling

pathway. **C** GO enrichment showed that some of the up-regulated genes were enriched in the type-I IFN signaling pathway. **D** GSEA indicated that a portion of the up-regulated genes were enriched in the type-I IFN signaling pathway. **E** ssGSEA showed significant upregulation of genes related to type-I IFN response pathway. **F** Up-regulated genes that were enriched in the type-I IFN response pathway

STAT1 and GBP1 are another two kinds of ISG and show inhibitory function in osteogenesis [34]. Fracture callus remodeling and membranous ossification of STAT1-deficient mice is much more faster than wild mice [35]. Similarly, in our study, overexpression of FKBP5 also promoted callus remodeling in mice of bone defect models. Mechanistically, STAT1 suppresses promoter activity of Osterix and inactivates RUNX2 via binding to it [36]. These data indicates that ISG, including but not limited to STAT1, GBP1, and IFIT2, are not only markers of IFN signaling, but also participate in the inhibition of osteogenesis. Therefore, regulating the expression of ISG may an effective approach to promote osteogenic differentiation.

Previous articles report that FKBP5, as a key factor in immune-related pathway, is involved in the regulation of

immune system. For example, deletion of FKBP5 results in increase in the number of CD8 + T, CD4 + T, NKT, and CD4 + NKT cells of mouse model of liver cancer, for which inhibiting tumor progress [37]. Furthermore, knockout of FKBP5 increases the risk of influenza A virus (IAV) infection. combination of FKBP5 and IκBα kinase (IKK) is an essential step for retinoic acid-inducible gene I (RIG-I) induced innate immune response and ISG expression [38]. However, in our experiment, knockdown of FKBP5 results in an increase in ISG expression, including IFIT2, which expands the regulation relationship of ISG expression by FKBP5. The reason for this contradiction might be that we applied different cell types and stimulatory factors. Of course, the specific regulatory mechanism still needs further exploration.

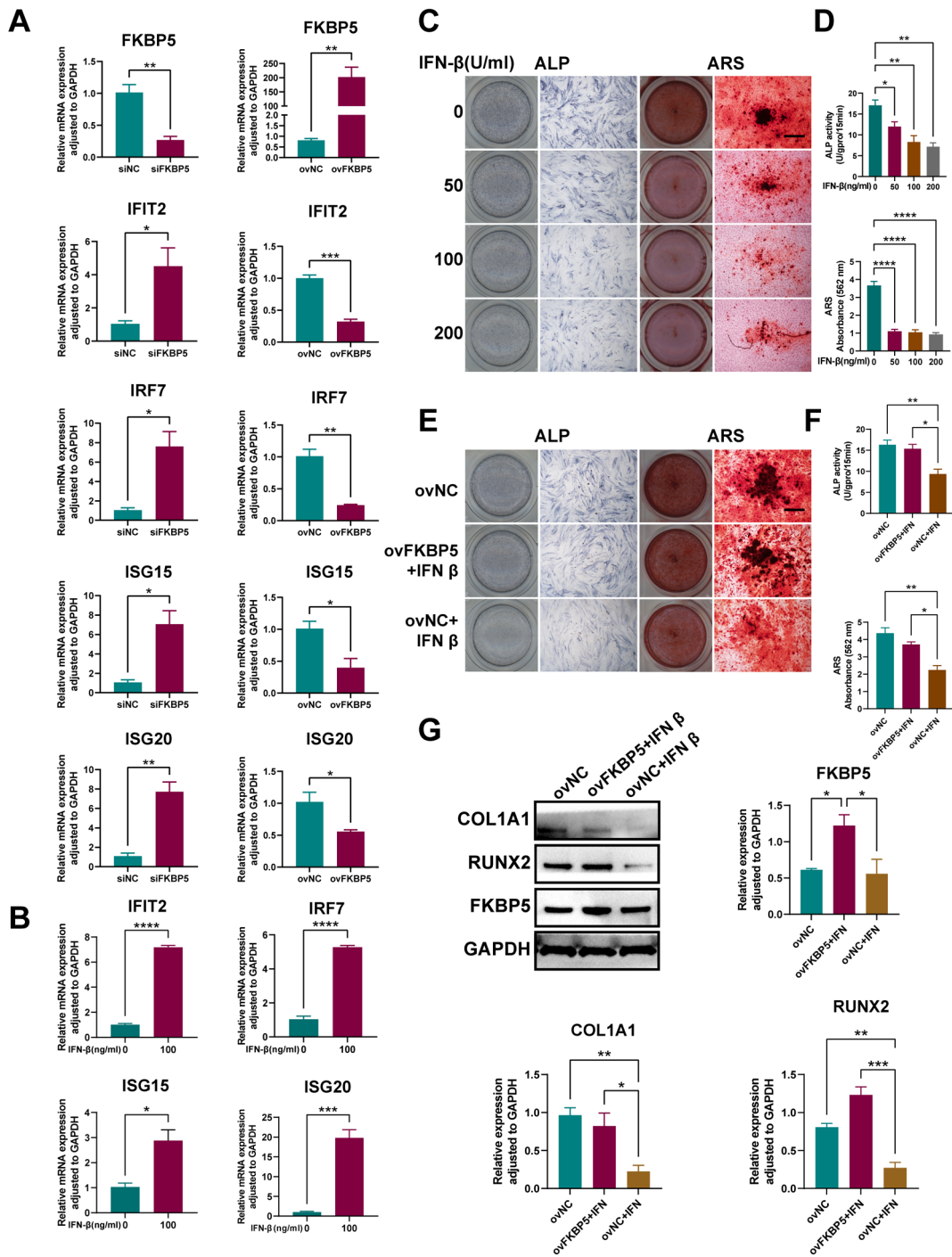


Fig. 5 FKBP5 mitigates the effect of IFN β on reducing osteogenesis of BMSCs. **A** FKBP5 knockdown resulted in amplification of ISG transcription, while overexpression of FKBP5 down-regulated these ISG. **B** IFN β up-regulated the expression of ISG of BMSCs. **C** IFN β impaired osteogenic potential of BMSCs, as evidenced by reduced ALP staining and ARS (scale bar: 200 μ m). **D** Quantitative analysis of ALP activity and ARS. **E** IFN β weakened ALP staining and ARS

of BMSCs, but this effect could be alleviated by FKBP5 overexpression (scale bar: 200 μ m). **F** Quantitative analysis of Fig. **E**. **G** IFN β down-regulated protein expression of COL1 A1 and RUNX2 of BMSCs, whereas overexpression of FKBP5 relatively upregulated the protein of these two markers. All experiments were performed independently and repeated three times

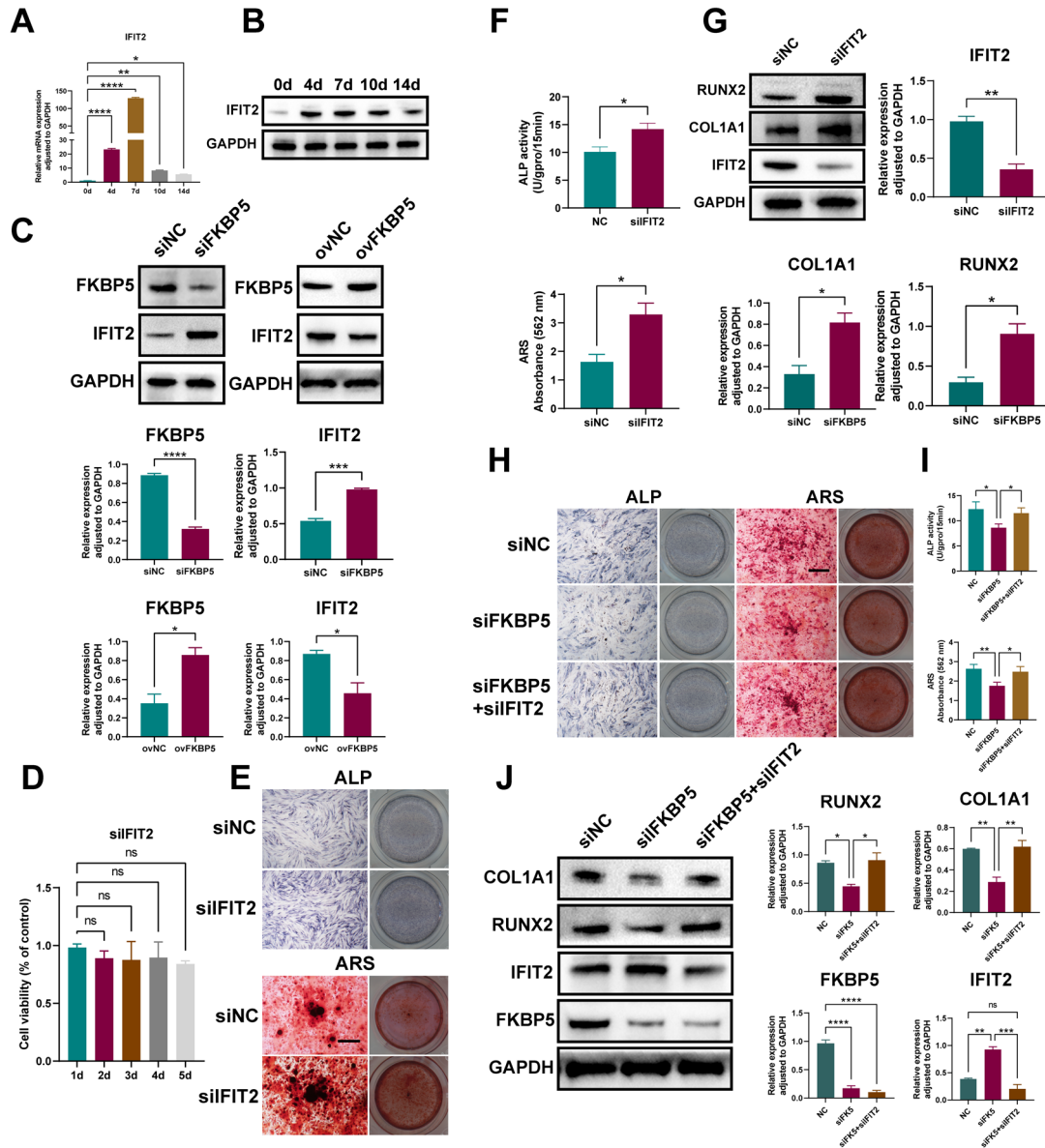


Fig. 6 FKBP5 modulates the osteogenesis of BMSCs through IFIT2. **A** The mRNA of IFIT2 raised during osteogenic induction of BMSCs, and peaked on day 7. **B** The protein of IFIT2 increased during osteogenic induction of BMSCs, which displayed a rising trend analogous to mRNA. **C** Knockdown of FKBP5 up-regulated IFIT2 protein, whereas overexpression of FKBP5 down-regulated it. **D** Evaluation of viability of BMSCs transfected with siIFIT2. **E** Knockdown of IFIT2 resulted in elevated ALP staining and ARS intensity of BMSCs (scale bar: 200 μm). **F** Quantitative analysis of Fig. **E**. **G** siRNA targeting IFIT2 suc-

cessfully knocked down IFIT2 protein and up-regulated the protein level of RUNX2 and COL1 A1. **H** siRNA against FKBP5 weakened ALP and ARS of BMSCs, while this effect could be rescued by knock-down of IFIT2 (scale bar: 200 μm). **I** Quantitative analysis of Fig. **H**. **J** siRNA against FKBP5 down-regulated the protein expression of COL1 A1 and RUNX2, while knockdown of IFIT2 up-regulated the expression of these two proteins. All experiments were performed independently and repeated three times

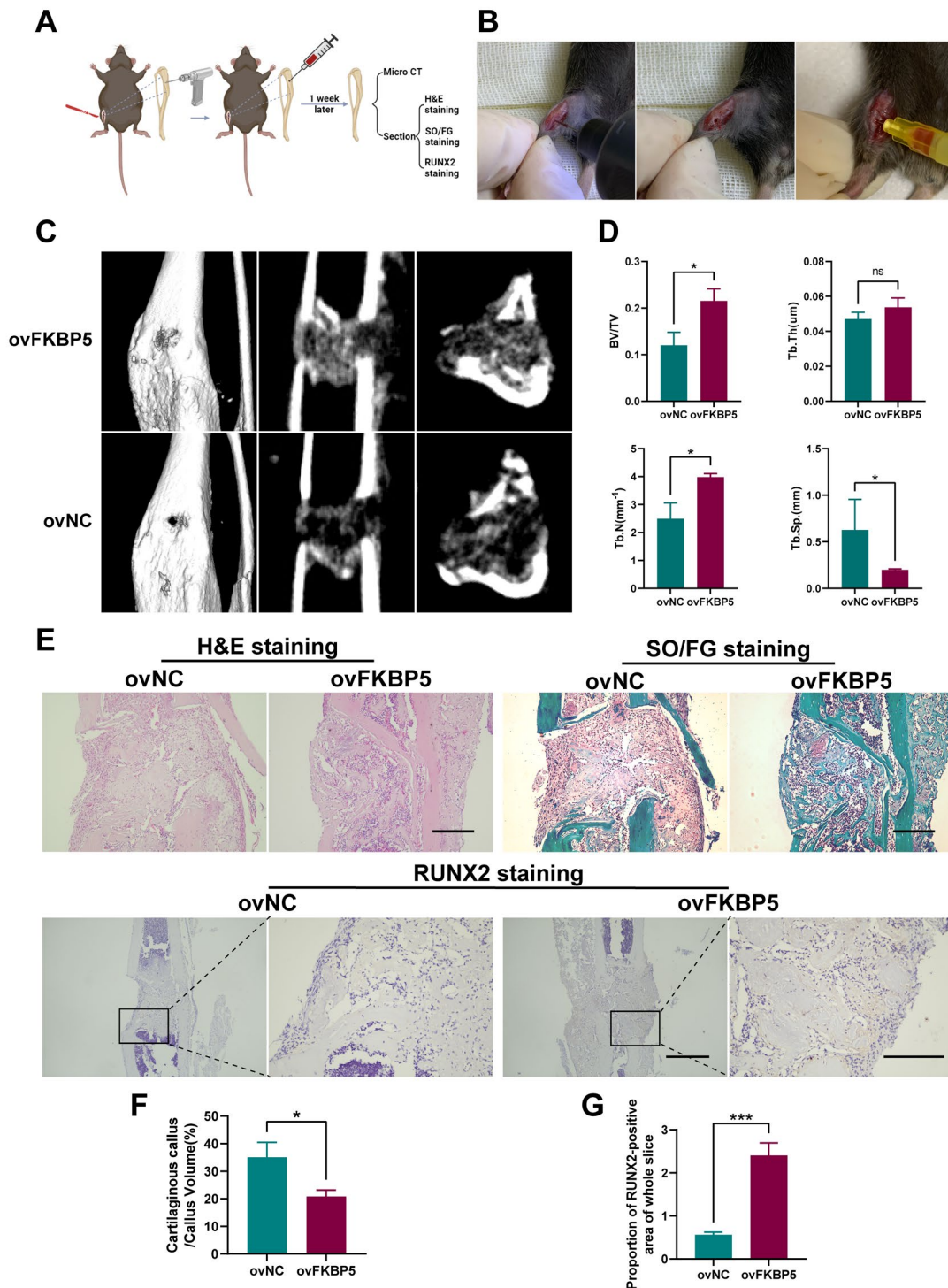


Fig. 7 Overexpression of FKBP5 promotes bone healing in vivo. **A** After successfully anesthetizing C57 mice, the skin that covered tibia was incised. The muscle was separated to expose tibia, and a hole was made using drilling machine. Subsequently, lentivirus overexpressing FKBP5 was injected into the bone hole, and the incision was sutured. One week later, the tibia was harvested for micro-CT scan and histological sectioning. **B** Illustration of tibial drilling and lentivirus injection. **C** Micro-CT images showed that under the same window

width and window level, ovFKBP5 group exhibited more amount of visible callus. **D** Quantitative analysis based on micro-CT images. **E** H&E (scale bar: 200 μm), SO/FG (scale bar: 200 μm), and RUNX2 staining (left scale bar: 200 μm, right scale bar: 50 μm) of the paraffin sections. **F** Quantification of Cartilaginous callus volume per total callus volume. **G** Quantification of positive area of RUNX2. All experiments were performed independently and repeated three times, $n = 5$

Conclusions

In summary, we discovered that FKBP5 promoted osteogenesis of BMSCs both in vitro and in vivo and confirmed that its function was achieved by blocking type-I IFN response and inhibiting IFIT2 expression. These results indicated that FKBP5 had the potential to serve as a target for inhibiting immune-related bone loss and promoting bone healing.

Supplementary Information The online version contains supplementary material available at <https://doi.org/10.1007/s00018-025-05754-1>.

Acknowledgements Not applicable.

Author contributions Study design, experiments, data analysis, article writing were completed by Jun Tang. Ming Li and Yuanquan Chen performed parts of the experiments and article revision. Yuwei Liang and Yuxi Li checked and revised the article. Qing Ning, Wenbin Yan, Hao Deng and Huatao Liu helped to perform experiments in vivo and in vitro. Lin Huang was responsible for conception and design of the work.

Funding This work was supported by grants from the Natural Science Foundation of Guangdong Province (2022 A1515012305, 2021 A1515111013) and Guangzhou Municipal Science and technology project (202201010881).

Data availability The data presented in current study are included in the article and supplemental material. The public datasets (GSE178679, GSE183931, GSE80614, GSE147390) used in this article are deposited in the NCBI Gene Expression Omnibus and are accessible through GEO Series accession number (<https://www.ncbi.nlm.nih.gov/geo/que/ry/acc.cgi>).

Declarations

Ethics approval and consent to participate This study was performed in line with the principles of the Declaration of Helsinki. Approval was granted by the Ethics Committee of Sun Yat-sen Memorial Hospital of Sun Yat-sen University (No. SYSKY-2024-861-01, Date: 2024.10.16) and Institutional Animal Care and Use Committee of Sun Yat-Sen University (No. SYSU-IACUC-2024-000014, Date: 2023.10.12).

Consent for publication Not applicable.

Competing interests The authors declare no competing interests.

Open Access This article is licensed under a Creative Commons Attribution-NonCommercial-NoDerivatives 4.0 International License, which permits any non-commercial use, sharing, distribution and reproduction in any medium or format, as long as you give appropriate credit to the original author(s) and the source, provide a link to the Creative Commons licence, and indicate if you modified the licensed material. You do not have permission under this licence to share adapted material derived from this article or parts of it. The images or other third party material in this article are included in the article's Creative Commons licence, unless indicated otherwise in a credit line to the material. If material is not included in the article's Creative Commons licence and your intended use is not permitted by statutory regulation or exceeds the permitted use, you will need to obtain permission

directly from the copyright holder. To view a copy of this licence, visit <http://creativecommons.org/licenses/by-nc-nd/4.0/>.

References

- (1993) Consensus development conference: diagnosis, prophylaxis, and treatment of osteoporosis. *Am J Med* 94(6). [https://doi.org/10.1016/0002-9343\(93\)90218-e](https://doi.org/10.1016/0002-9343(93)90218-e)
- Mattias L (2019) Treating osteoporosis to prevent fractures: current concepts and future developments. *J Intern Med* 285(4). <http://doi.org/10.1111/joim.12873>
- Hadjidakis DI, Androulakis II (2006) Bone remodeling. *Ann N Y Acad Sci* 1092(Dec):385–p396
- Rossella C, Federica B, Rosita C, Antonio AA, Sandro LV, Aldo C (2019) Osteoporosis from an endocrine perspective: the role of hormonal changes in the elderly. *J Clin Med* 8. <https://doi.org/10.3390/jcm8101564>
- Maruotti N, Corrado A, Cantatore FP (2014) Osteoporosis and rheumatic diseases. *Reumatismo* 66(2):125–35. <https://doi.org/10.4081/reumatismo.2014.785>
- Boskey AL, Coleman R (2010) Aging and bone. *J Dent Res* 89(12). <https://doi.org/10.1177/0022034510377791>
- Szulc P, Seeman E (2009) Thinking inside and outside the envelopes of bone: dedicated to PDD. *Osteoporos Int* 20(8). <https://doi.org/10.1007/s00198-009-0994-y>
- Zhong W, Mark G, Michael S (2008) RNA-Seq: a revolutionary tool for transcriptomics. *Nat Rev Genet* 10(1). <https://doi.org/10.1038/nrg2484>
- Li C, Kaikai S, Nicholas D, Weimin Q, Florence F, Louise Himmelstrup Dreyer N, Michaela T, Justyna Magdalena K, Ming D, Christina Møller A, Thomas A, Levin, Moustapha K (2023) KIAA1199 deficiency enhances skeletal stem cell differentiation to osteoblasts and promotes bone regeneration. *Nat Commun* 14(1). <https://doi.org/10.1038/s41467-023-37651-1>
- Lifang H, Chong Y, Dong C, Zixiang W, Shujing L, Yu Z, Zizhan H, Shuyu L, Xia X, Zhihao C, Yi Z, Airong Q (2021) MACF1 promotes osteoblast differentiation by sequestering repressors in cytoplasm. *Cell Death Differ* 28(7). <https://doi.org/10.1038/s41418-021-00744-9>
- Zannas A, Jia M, Hafner K, Baumert J, Wiechmann T, Pape J, Arloth J, Ködel M, Martinelli S, Roitman M, Röh S, Haehle A, Emeny R, Iurato S, Carrillo-Roa T, Lahti J, Räikkönen K, Eriksson J, Drake A, Waldenberger M, Wahl S, Kunze S, Lucae S, Bradley B, Gieger C, Hausch F, Smith A, Ressler K, Müller-Myhsok B, Ladwig K, Rein T, Gassen N, Binder E (2019) Epigenetic upregulation of FKBP5 by aging and stress contributes to NF- κ B-driven inflammation and cardiovascular risk. *Proc Natl Acad Sci USA* 116(23):11370–11379. <https://doi.org/10.1073/pnas.1816847116>
- Deng Z, Ng C, Inoue K, Chen Z, Xia Y, Hu X, Greenblatt M, Perinis A, Zhao B (2020) Def6 regulates endogenous type-I interferon responses in osteoblasts and suppresses osteogenesis. *eLife*. <https://doi.org/10.7554/eLife.59659>
- Ming L, Zhongyu X, Peng W, Jinteng L, Wenjie L, Su'an T, Zhenhua L, Xiaohua W, Yanfeng W, Huiyong S (2018) The long noncoding RNA GAS5 negatively regulates the adipogenic differentiation of MSCs by modulating the miR-18a/CTGF axis as a CeRNA. *Cell Death Dis* 9(5). <https://doi.org/10.1038/s41419-018-0627-5>
- Peng W, Yuxi L, Lin H, Jiewen Y, Rui Y, Wen D, Biling L, Lie D, Qingqi M, Liangbin G, Xiaodong C, Jun S, Yong T, Xin Z, Jingyi H, Jichao Y, Keng C, Zhaopeng C, Yanfeng W, Huiyong S (2013) Effects and safety of allogeneic mesenchymal stem cell intravenous infusion in active ankylosing spondylitis patients who failed

- NSAIDs: a 20-week clinical trial. *Cell Transpl* 23(10). <https://doi.org/10.3727/096368913x667727>
15. Jing H, Xia H, Liwen Z, Yuxin Z, Huan Z, Li N, Xiaoxiao P, Hongmei Z (2023) MiR-199a-5P promotes osteogenic differentiation of human stem cells from apical papilla via targeting IFIT2 in apical periodontitis. *Front Immunol* 14. <https://doi.org/10.3389/fimmu.2023.1149339>
 16. Xiao-Yu T, Biao Z, Wen-Can F, Xiang-Bin Z, Ning W, Hong L, Ning W, Jin L (2024) FKBP5 regulates the osteogenesis of human Adipose-derived mesenchymal stem cells. *Curr Med Sci* 44(6). <https://doi.org/10.1007/s11596-024-2941-8>
 17. Ankit S, Harsh S, Benjamin NL, Michael L (2020) Mechanisms of bone development and repair. *Nat Rev Mol Cell Biol* 21(11). <https://doi.org/10.1038/s41580-020-00279-w>
 18. Garnero P, Sornay-Rendu E, Chapuy MC, Delmas PD (1996) Increased bone turnover in late postmenopausal women is a major determinant of osteoporosis. *J Bone Min Res* 11(3). <https://doi.org/10.1002/jbmr.5650110307>
 19. Qing Z, Xinran L, Chuanying Y, Yu X (2022) Macrophages and bone marrow-derived mesenchymal stem cells work in concert to promote fracture healing: a brief review. *DNA Cell Biol* 41(3). <https://doi.org/10.1089/dna.2021.0869>
 20. Maria Teresa V, Luca DC, Monica M (2016) Osteogenic differentiation in healthy and pathological conditions. *Int J Mol Sci* 18(1). <https://doi.org/10.3390/ijms18010041>
 21. Masayuki T, Hiroshi T (2019) Osteoimmunology: evolving concepts in bone-immune interactions in health and disease. *Nat Rev Immunol* 19(10). <https://doi.org/10.1038/s41577-019-0178-8>
 22. Takako N-K, Hans-Jürgen G, Eriko S, Noriko K, Kazuo O, Shin-ichiro S, Ayako S, Tomomi S, Kojiro S, Toshiyuki T, Hiroshi T (2015) Immune complexes regulate bone metabolism through FcRγ signalling. *Nat Commun* 6(0). <https://doi.org/10.1038/ncomms7637>
 23. Ulrike H, Stefanie L, René CP, Yoann R, Sabine F, Khaled A, Holger B, Anja L, Carolien K, Wolfgang AB, Katharina D, Franziska G, Vivianne M, Lars K, Gerhard K, Roland K, Falk N, René T, Martin EMH, Hans S, Ulrich, Georg S (2015) Glycosylation of Immunoglobulin G determines osteoclast differentiation and bone loss. *Nat Commun* 6(0). <https://doi.org/10.1038/ncomms7651>
 24. Cenci S, Weitzmann MN, Roggia C, Namba N, Novack D, Woodring J, Pacifici R (2000) Estrogen deficiency induces bone loss by enhancing T-cell production of TNF-α. *J Clin Invest* 106. <https://doi.org/10.1172/jci11066>
 25. Irene EM (2012) Osteoporosis and fractures in systemic lupus erythematosus. *Arthritis Care Res (Hoboken)* 64(1). <https://doi.org/10.1002/acr.20568>
 26. Antonios P, Miriam W, Edward V (2022) Emerging concepts of type I interferons in SLE pathogenesis and therapy. *Nat Rev Rheumatol* 18(10). <https://doi.org/10.1038/s41584-022-00826-z>
 27. Lin G, Jane L, Jennifer A, Andrew M, Richard John I (2020) IFNβ signaling inhibits osteogenesis in human SLE bone marrow. *Lupus* 29(9). <https://doi.org/10.1177/0961203320930088>
 28. Antonios P, Paul E, Edward V (2017) Type I interferon-mediated autoimmune diseases: pathogenesis, diagnosis and targeted therapy. *Rheumatology (Oxford)* 56(10). <https://doi.org/10.1093/rheumatology/kew431>
 29. Takayanagi H, Sato K, Takaoka A, Taniguchi T (2005) Interplay between interferon and other cytokine systems in bone metabolism. *Immunol Rev* 208:181–193. <https://doi.org/10.1111/j.0105-2896.2005.00337.x>
 30. Woeckel VJ, Eijken M, van de Peppel J, Chiba H, van der Eerden BCJ, van Leeuwen JPTM (2011) Evidence of vitamin D and interferon-β cross-talk in human osteoblasts with 1α,25-dihydroxyvitamin D3 being dominant over interferon-β in stimulating mineralization. *J Cell Physiol* 227(6). <https://doi.org/10.1002/jcp.23009>
 31. Woeckel V J, Koedam M, van de Peppel J, Chiba H, van der Eerden BCJ, van Leeuwen JPTM (2011) Evidence of vitamin D and interferon-β cross-talk in human osteoblasts with 1α,25-dihydroxyvitamin D3 being dominant over interferon-β in stimulating mineralization. *J Cell Physiol* 227(9). <https://doi.org/10.1002/jcp.24020>
 32. Volker F, Sen GC (2010) The ISG56/IFIT1 gene family. *J Interferon Cytokine Res* 31(1). <https://doi.org/10.1089/jir.2010.0101>
 33. Lian-Feng L, Jiahui Y, Yuexiu Z, Qian Y, Yongfeng L, Lingkai Z, Jinghan W, Su L, Yuzi L, Yuan S, Hua-Ji Q (2017) Interferon-Inducible oligoadenylate synthetase-like protein acts as an antiviral effector against classical swine fever virus via the MDA5-mediated type I interferon-signaling pathway. *J Virol* 91(11). <https://doi.org/10.1128/jvi.01514-16>
 34. Bai S, Mu Z, Huang Y, Ji P (2018) Guanylate binding protein 1 inhibits osteogenic differentiation of human mesenchymal stromal cells derived from bone marrow. *Sci Rep* 8(1):1048. <https://doi.org/10.1038/s41598-018-19401-2>
 35. Tajima K, Takaishi H, Takito J, Tohmonda T, Yoda M, Ota N, Kosaki N, Matsumoto M, Ikegami H, Nakamura T, Kimura T, Okada Y, Horiuchi K, Chiba K, Toyama Y (2010) Inhibition of STAT1 accelerates bone fracture healing. *J Orthop Research: Official Publication Orthop Res Soc* 28(7):937–941. <https://doi.org/10.1002/jor.21086>
 36. Kim S, Koga T, Isobe M, Kern B, Yokochi T, Chin Y, Karsenty G, Taniguchi T, Takayanagi H (2003) Stat1 functions as a cytoplasmic attenuator of Runx2 in the transcriptional program of osteoblast differentiation. *Genes Dev* 17(16):1979–1991. <https://doi.org/10.1101/gad.1119303>
 37. Chuantao Z, Xiang C, Lian F, Zhiyi H, Deti P, Wenjun F, Yufeng X (2021) The deficiency of FKBP-5 inhibited hepatocellular progression by increasing the infiltration of distinct immune cells and inhibiting obesity-associated gut microbial metabolite. *J Gastrointest Oncol* 12(2). <https://doi.org/10.1101/gad.1119303>
 38. Wenzhuo H, Lingyan W, Shitao L (2020) FKBP5 regulates RIG-I-Mediated NF-κB activation and influenza A virus infection. *Viruses* 12(6). <https://doi.org/10.1101/gad.1119303>

Publisher's note Springer Nature remains neutral with regard to jurisdictional claims in published maps and institutional affiliations.